Is the Function of the cdc2 Kinase Subunit Proteins Tuned by Their Propensities To Oligomerize? Conformational States in Solution of the cdc2 Kinase Partners $p13^{suc1}$ and $p9^{cksphy}$ †

Catherine Birck, Patrice Vachette,‡ Martin Welch, Peter Swarén, and Jean-Pierre Samama*

Groupe de Cristallographie Biologique du Laboratoire de Pharmacologie et de Toxicologie Fondamentales du CNRS, UPR 8221, 205 route de Narbonne, 31077 Toulouse, France

Received September 14, 1995; Revised Manuscript Received January 2, 1996⊗

ABSTRACT: The cdc2 kinase subunit (cks) proteins play an essential function in the control of mitosis through their molecular complexes with the cdc2 kinase. In this work, we characterize the conformational state(s) in solution of the cks proteins $p13^{suc1}$ from *Schizosaccharomyces pombe* and $p9^{cksphy}$ from *Physarum polycephalum*. Monomers of $p13^{suc1}$ and $p9^{cksphy}$ were found to be markedly nonglobular, presumably with a long, nonfolded C-terminal moiety. This was in contrast to the previously published structure of $p13^{suc1}$, derived from crystallographic studies on a zinc-promoted $p13^{suc1}$ dimer, in which the individual $p13^{suc1}$ subunits had a globular conformation. This disparity was resolved when we found that the globular $p13^{suc1}$ fold undergoes a conformational transition into nonglobular monomers upon dissociation of the dimers following chelation of the zinc ions by ethylenediaminetetraacetic acid (EDTA). We also found that $p13^{suc1}$, but not $p9^{cksphy}$, forms stable dimers in the absence of metal ions. The topology of these EDTA-insensitive dimers likely resembles that of the human $p9^{ckshs2}$ protein, characterized by β4 strand exchange from each nonglobular monomer.

In the yeasts *Schizosaccharomyces pombe* and *Saccharomyces cerevisiae*, the serine/threonine kinase $p34^{cdc2/cdc28}$ (hereafter, cdc2) controls the G1/S and G2/M transitions, committing the cell to another cell cycle and to mitosis, respectively [reviewed in Pines (1993)]. In higher eukaryotic cells, cdc2 regulates just one step, the entry into mitosis. The other cell cycle transitions are controlled by kinases related to cdc2, known as the cyclin-dependent kinases (cdks). Recent work has shown that the cdks are activated when they form complexes with different types of cyclins (King *et al*., 1994). In the case of cdc2, the minimal unit required for kinase activity is a cdc2−cyclin B complex (Draetta & Beach, 1988; Solomon *et al*., 1990; Desai *et al*., 1992). The kinase activity of cdc2 is also regulated by the phosphorylation state of the conserved residues Thr14, Thr161, and Tyr15 (human cdc2 numbering) and by the association of the kinase with other, non-cyclin proteins [reviewed in Dunphy (1994) and Draetta (1993)]. These protein partners have been proposed to help in defining substrate specificity, affinity, and intracellular location of cdc2 (Kusubata *et al*., 1992; Brizuela *et al*., 1989; Booher *et al*., 1989). In *S. pombe*, among these partners, cdc2 associates with a small protein encoded by the *suc1* gene, isolated as a high-copy suppressor of certain temperature-sensitive *cdc2* mutants (Hayles *et al*., 1986a; Brizuela *et al*., 1987). Proteins homologous to $p13^{suc1}$ have been found in budding yeast, myxomycetes, mollusks, starfish, flowering plants, and vertebrates, suggesting that $p13^{suc1}$ plays an important role in the regulation of the cell cycle (Hadwiger *et al*., 1989; Birck *et al*., 1995; Colas *et al*., 1993; Azzi *et al*., 1994; John *et al*., 1991; Richardson *et al*., 1990). Collectively, these proteins form the cks family (for cdc2 kinase subunit). Members of the cks family are conserved at the primary structure level, displaying 51−81% identity to one another. The cks proteins of yeast species are larger, as a consequence of sequence insertions outside the conserved regions (Figure 1).

Not much is known about the function of the cks proteins. In *S. pombe*, deletion of the *suc1* gene is lethal (Hayles *et al*., 1986b). Overexpression of the cks proteins delays entry into mitosis, suggesting that these proteins play a role in controlling this process (Moreno *et al*., 1989; Richardson *et al*., 1990). *In vitro* studies have shown that $p13^{suc1}$ inhibits the phosphatase activity of cdc25 (Dunphy & Newport, 1989) and that it is not a substrate of cdc2 (Brizuela *et al*., 1987). It was also recently proposed that $p13^{suc1}$ may regulate two types of cdc2−cyclin complexes (Basi & Draetta, 1995). However, despite numerous investigations, the precise function(s) of the cks proteins remains enigmatic, and their regulatory properties remain undefined.

Possible insights into the function of the cks proteins followed the X-ray structure determination of the human $p9^{ckshs2}$ homologues. In the case of $p9^{ckshs2}$, the protein crystallized as a hexamer composed of three dimers. Each dimer is stabilized through the β4 strand exchange of the conserved HXPEPHILLFRX sequence (residues 60 → 71, human numbering) from each nonglobular monomer (Parge *et al*., 1993). These workers proposed that the cks proteins might act as a "hub" for the oligomerization of the cdks. In the same work, monomeric, dimeric, and hexameric forms of $p9^{ckshs2}$ were found to interconvert in solution, in an ionic strength- and calcium-dependent manner. This, and the

† This work was supported by the Association pour la Recherche sur la Cancer (ARC) Grant 6564. C.B. has a fellowship from ARC. M.W. is supported by a postdoctoral fellowship from ARC.

* Corresponding author.

‡ LURE (CNRS-CEA-MENESRIP), Bat. 209D, Centre Universitaire Paris-Sud, 91405 Orsay, France.

⊗ Abstract published in *Advance ACS Abstracts,* April 1, 1996.

S0006-2960(95)02199-4 CCC: $12.00

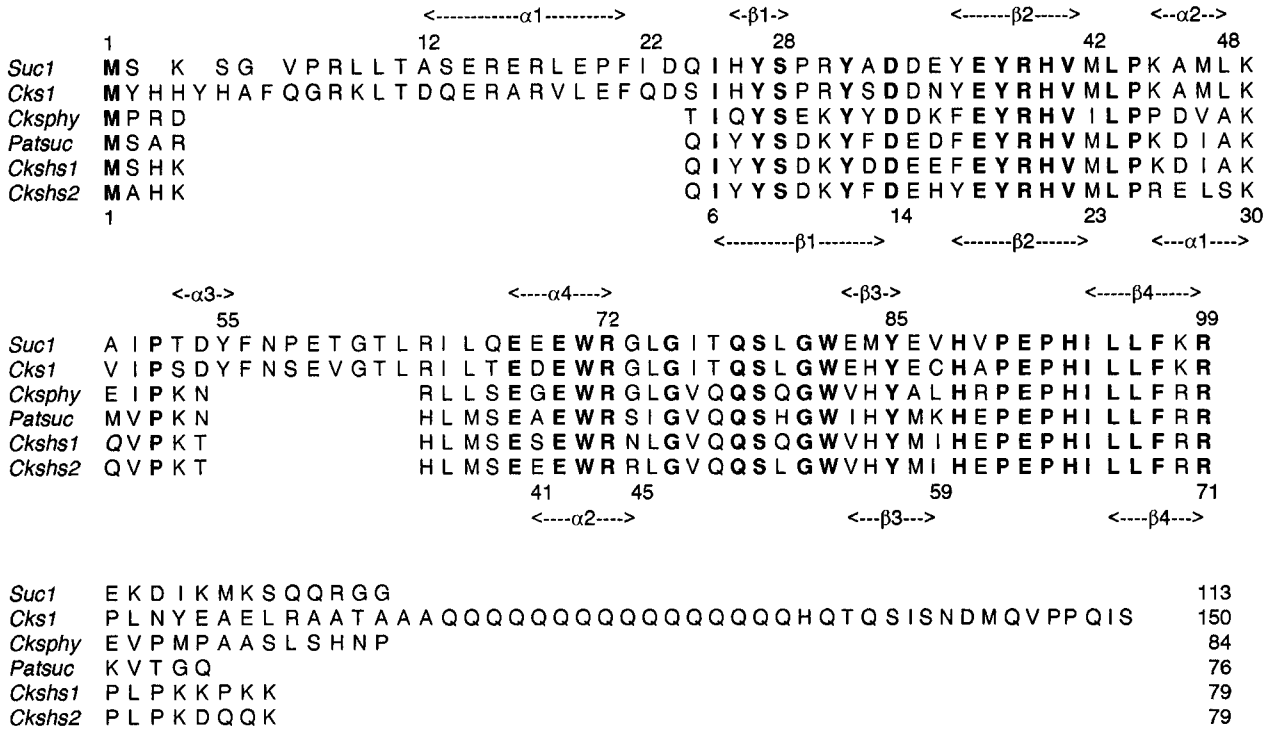

FIGURE 1: Alignment of the *Physarum* cksphy amino acid sequence with the known cks homologues: *S. cerevisiae* cks1 (Hadwiger *et al*., 1989); *S. pombe* suc1 (Hindley *et al*., 1987); *Patella vulgata* patsuc (Colas *et al*., 1993); human ckshs1 and ckshs2 (Richardson *et al*., 1990) and secondary structure assignments. The conserved residues are indicated in boldface type and the numberings of amino acids refer either to the $p13^{suc1}$ sequence (top) or human sequences (bottom). The positions of α helices and β strands were from the suc1 and ckshs2 crystal structures (Endicott *et al*., 1995a; Parge *et al*., 1993).

peculiar fold of each monomer in the dimer, led to the suggestion that refolding of the C-terminal β4 strand onto the N-terminal globular domain would lead to globular monomers. The $p13^{suc1}$ protein crystallized as a dimer, whose formation was sharply dependent on the composition of the medium (Endicott *et al*., 1995a). However, the topology of this zinc-promoted $p13^{suc1}$ dimer appears quite different from that observed in $p9^{ckshs2}$. Each $p13^{suc1}$ polypeptide chain has a globular structure. Dimer formation involves two zinc-mediated interactions and six charged-residue interactions between monomers.

The properties of human $p9^{ckshs2}$ and $p9^{ckshs1}$ (Parge *et al*., 1993; Arvai *et al*., 1995) contrast with those of the cks protein $p9^{cksphy}$, which comes from the myxomycete *Physarum polycephalum* (a syncytium dividing with perfect synchrony). In spite of having 62% sequence identity to the human proteins (Figure 1), $p9^{cksphy}$ was found to be a stable, monodispersed monomeric species (Birck *et al*., 1995). In the same work, preliminary data on the solution state of monomeric $p13^{suc1}$ proteins were presented.

In this paper, we extend our earlier results with $p9^{cksphy}$ and $p13^{suc1}$ by defining, for each protein, its conformation in solution and its ability to interconvert between monomeric and dimeric forms.

MATERIALS AND METHODS

Expression and Purification of Recombinant cks Proteins. The $p9^{cksphy}$ and $p13^{suc1}$ proteins were produced in *Escherichia coli* and purified as previously described (Birck *et al*., 1995). Proteins were analyzed on SDS-containing 8−20% gradient polyacrylamide gels (Laemmli, 1970) and stained wth Coomassie Blue R250 or silver stain (Bloom *et al*., 1987).

N-Terminal Amino Acid Sequencing. The amino acid analysis of the recombinant $p9^{cksphy}$ protein (in 10 mM ammonium bicarbonate, pH 7.2) revealed the absence of the initial methionine and confirmed the first 15 amino acids (carried out at the ICGM laboratory, Paris). The concentration of the $p9^{cksphy}$ solution was determined by quantitative amino acid analysis which allowed the calculation of the extinction coefficient ($\epsilon_{1\%/cm} = 18.6$).

Mass Spectrometry Analysis. For analysis by electrospray ionization mass spetrometry, the $p9^{cksphy}$ and $p13^{suc1}$ monomers were dialyzed against 10 mM ammonium bicarbonate (pH 7.2). The experimental $p9^{cksphy}$ M_r (9 592) corresponded to its theoretical M_r (9 936) minus the initial methionine and the last two C-terminal proline and asparagine residues. The experimental $p13^{suc1}$ M_r (13 316) corresponded to its theoretical M_r (13 447) minus the initial methionine.

Small Angle X-ray Scattering (SAXS). For SAXS measurements, $p13^{suc1}$ proteins were dialyzed against either 50 mM Tris-HCl (pH 8.5) and 250 mM NaCl or 10 mM Tris-HCl (pH 7.4) and 200 mM NaCl. In the latter case, the proteins were concentrated to 1 mg/mL, mixed with 1 mM $ZnSO_4$ final concentration, and incubated for 15 min. The protein solution was then concentrated to 3 mg/mL, and one aliquot was mixed with 5 mM EDTA, final concentration, prior to SAXS measurements. The $p13^{suc1}$ concentration in each experiment was determined spectrophotometrically ($\epsilon_{1\%/cm} = 15.2$). The samples contained 1 mM DTT to eliminate the free radicals formed in solution under X-ray irradiation.

X-ray scattering curves were recorded on the small-angle scattering instrument D24 using synchrotron radiation at LURE-DCI, Orsay, France. The instrument (Depautex *et al*., 1987), the data acquisition system (Bordas *et al*., 1980) and the experimental protocols (Birck *et al*., 1995) have already been described.

The radius of gyration was derived from a Guinier analysis (Guinier & Fournet, 1955). The distance distribution func-

tion $p(r)$ was calculated using the program GNOM, version E4.2 (Svergun, 1992; Svergun *et al*., 1988). Due to the very low concentration of the solutions used, only estimates of the maximal molecular dimension (d_{max}) of the particles were obtained.

X-ray scattering patterns were computed from crystallographic coordinates using the program CRYSOL recently developed by Svergun and collaborators, which takes solvent effects into account through the contribution of a hydration layer surrounding the protein surface (Svergun *et al*., 1995). The electron density contrast of this external layer is an adjustable parameter when fitting an experimental scattering curve using crystallographic coordinates. In all calculations performed here, this parameter had a value corresponding to a hydration in the range 0.4−0.5 g of H_2O/g of protein.

Analytical Ultracentrifugation Measurements. Sedimentation velocity and sedimentation equilibrium experiments were performed at 20 °C on a Beckman Model XL-A analytical ultracentrifuge (IBS, Grenoble, France). In each experiment, three samples were run in a four-place AN60-TI rotor, using 12-mm double-sector cells with quartz windows. For velocity runs, the cells were filled with 400 μL of protein solution ($p13^{suc1}$ at 0.8 and 0.25 mg/mL, $p9^{cksphy}$ at 0.5 mg/mL) in one sector and 425 μL of 50 mM Tris-HCl (pH 7.3) and 100 mM NaCl in the other. Samples were centrifuged at 65 000 rpm, and 20 radial scans of absorbance at 278 nm were taken at 12-min intervals throughout the 4.5-h duration of the experiment. The computer program XLAVEL (Beckman) was used to analyze the data and determine the sedimentation coefficient (s). The s determination was based on an s value estimated for a specific scan with the equation $s = \ln (r_{infl}/r_0)/\bar{\omega}^2 t$, where s is the observed sedimentation coefficient, r_{infl} is the radial position of the inflection point for the sedimenting boundary location, r_0 is the radial position of the meniscus, $\bar{\omega}$, is the radial rotor velocity, and t is the time. The program plots $\ln (r_{infl}/r_0)$ versus $\bar{\omega}^2 t$ and calculates the best s value, reported in Svedbergs (S, 10^{-13} s^{-1}). The value of s was corrected to standard conditions of water at 20 °C. The equilibrium runs were performed for 18 h at 35 000 rpm, the double-sector cells were filled with 110 μL of protein solution (at 0.5 or 0.9 mg/mL for $p13^{suc1}$ and at 0.4 mg/mL for $p9^{cksphy}$) in one sector and with 125 μL of 50 mM Tris (pH 7.3) in the other. The concentration distributions were then analyzed by fitting appropriate mathematical models using the XLA/EQUASSOC analysis software supplied by Beckman. The EQUASSOC program calculates the association constants (K) and then permits the analysis of associating solutes containing monomers, dimers, trimers, and tetramers. The four parameters that are determined are M_1, the monomer molecular weight, and the logs of K_2, K_3, and K_4. A curve-fitting algorithm is used to obtain results with the equilibrium equations

$$C_r = C_1 + K_2(C_1)^2 + K_3(C_1)^3 + K_4(C_1)^4 \qquad (1)$$

$$\ln C_1/C_0 = [\bar{\omega}^2 M_1(1 - \rho\nu)/2RT](r^2 - r_0^2) \qquad (2)$$

In these equations, C_r is the total concentration of reversible self-associating protein at any radial position, r, after attaining sedimentation equilibrium. C_1 is the monomer concentration; C_0 is the concentration at radial reference position r_0, ρ is the solvent density, ν is the partial specific volume, R is the gas constant, and T is the absolute temperature. Data were analyzed according to different possible equilibrium models. The best fit of the absorbance versus radial distance data, using nonlinear regression, was found when assuming a single, ideal, nonassociating molecule. The knowledge of s, ν, and M_r allowed the calculation of the frictional coefficient

$$f = M_r(1 - \rho\nu_{exp})/Ns \qquad (3)$$

where N is Avogadro's number. The theoretical frictional coefficient for a particle composed of a sphere attached to an ellipsoid was calculated by modifying the equations given by Cantor and Schimmel (1980) for a cluster of identical subunits. The frictional coefficient f_0 of a hydrated sphere ($f_0 = 6\pi\eta R_h$) was calculated with $V_h = (M_r\ \nu_{exp}/0.602) \times 1.2$, where η is the viscosity of the medium, R_h is the hydrodynamic radius, and V_h is the hydrated volume of the protein (assuming 0.2 mg/mL hydration).

FPLC Size-Exclusion Chromatography. Analytical size-exclusion chromatography measurements were performed at 4 °C on a Superdex 75 10/30 column (Pharmacia). The column was equilibrated with 10 mM Tris-HCl (pH 7.4) and 200 mM NaCl or with 10 mM Tris-HCl (pH 7.4), 200 mM NaCl, and 1 mM $ZnSO_4$ or with 10 mM Tris-HCl (pH 7.4), 200 mM NaCl, 1 mM $ZnSO_4$, and 5 mM EDTA, at a flow rate of 0.5 mL/min (0.5-mL fractions). Volumes of 50 μL at 1 mg/mL protein were injected. The $p13^{suc1}$ and $p9^{cksphy}$ proteins were incubated for 30 min in the conditions corresponding to the elution buffer before injection on the fast protein liquid chromatography (FPLC) column. The column was calibrated using bovine serum albumin (M_r = 67 000, R_s = 35.5 Å), ovalbumin (M_r = 43 000, R_s = 30.5 Å), chymotrypsinogen B (M_r = 25 000, R_s = 20.9 Å), and ribonuclease A (M_r = 13 700, R_s = 16.4 Å) from the Pharmacia low molecular weight calibration kit.

Denaturation and Renaturation of EDTA-Insensitive $p13^{sucl}$ Dimers. Pure $p13^{sucl}$ dimers (250 μg) were denatured in 100 μL of 50 mM Tris-HCl (pH 8.5) and 6 M guanidinium chloride for 12 h at 4 °C. Renaturation was initiated by a rapid 30-fold dilution in 10 mM Tris-HCl (pH 7.4), 200 mM NaCl, and 150 mM L-arginine, with vigorous mixing for 20 s (Goldberg *et al*., 1991). The refolded protein was then dialyzed twice against the renaturing buffer and once against 10 mM Tris-HCl (pH 7.4) and 200 mM NaCl. After concentration to 1 mg/mL using Centricon 10 (Amicon), the renatured protein was mixed with 1 mM $ZnSO_4$ final concentration and incubated for 30 min before analysis by FPLC.

RESULTS

Conformational States of the Monomeric $p9^{cksphy}$ and $p13^{sucl}$ Proteins: (i) Analytical Ultracentrifugation. As a first step, we wanted to define the molecular envelope of the $p9^{cksphy}$ and $p13^{suc1}$ monomers in solution. To do this, we carried out analytical ultracentrifugation experiments to obtain a suitable number of parameters and calculate the frictional coefficient (f) of the proteins. This coefficient is directly related to the shape of the molecule. Two types of experiment were performed. First, from sedimentation velocity runs, the sedimentation coefficients (s) of $p9^{cksphy}$ and $p13^{suc1}$ monomers were measured to be 1.23 and 1.49 S, respectively (data not shown). These values are smaller than those of globular proteins of comparable size [e.g., ribonuclease A, M_r = 12 400, s = 1.85 S; lysozyme, M_r =

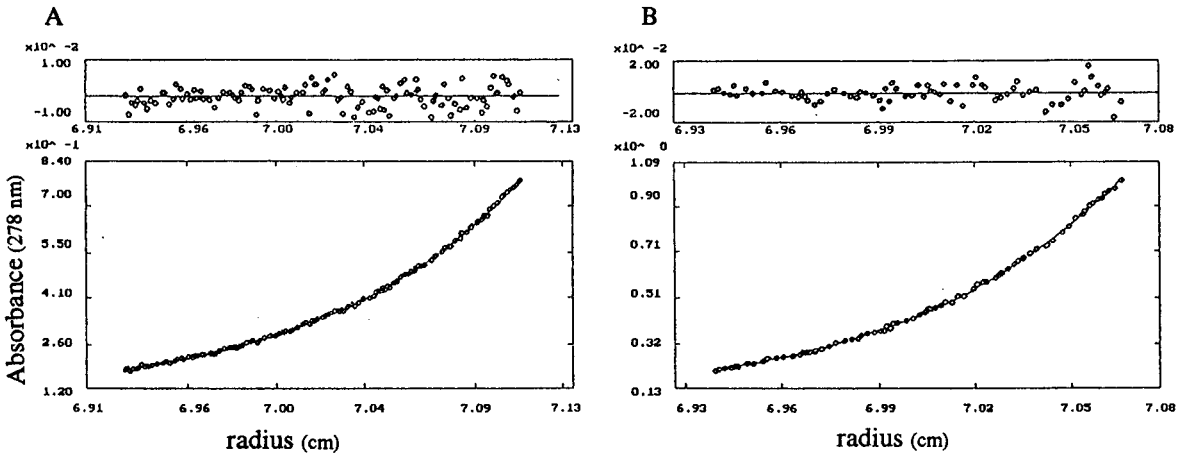

FIGURE 2: Sedimentation equilibrium data for p9^{cksphy} (A) and p13^{suc1} (B) monomers, plotted as absorbance as a function of r (lower graphs). Conditions were 50 mM Tris-HCl (pH 7.4), 100 mM NaCl, and 20 °C, and initial concentrations were 0.4 and 0.5 mg/mL for p9^{cksphy} and p13^{suc1}, respectively. The line in the lower graphs shows the best-fitting curve for the model which assumed the presence of a single, ideal, nonassociating solute, in line with the SAXS experiments (Birck *et al*., 1995). Upper graphs show that the distribution of the residuals of the fit is random.

Table 1: Molecular Weights and Sedimentation Parameters of cks Monomers

	mass spectrometry M_r (Da)	equilibrium M_r[a] (Da)	$s_{20,w}$ (S)	ν_{exp}[b] (cm^3/g)[b]	f ($\times 10^8$ g/s)	F[c]
p9^{cksphy}	9 592 ± 0.5	9 600	1.23	0.710	3.76	1.347
p13^{suc1}	13 316 ± 1.5	13 300	1.49	0.729	4.11	1.311

[a] Molecular masses calculated from sedimentation equilibrium by using the equilibration equation (eq 2): $\ln C_1/C_0 = [\bar{\omega}^2 M_1(1 - \rho\nu)/2RT](r^2 - r_0^2)$ with $\nu = 0.71$ and 0.72 cm^3/g for p9^{cksphy} and p13^{suc1}, respectively, and $\rho = 1.002$ g/cm^3. [b] Determined with eq 2 using fixed mass spectrometry M_r values. [c] Equal to f/f_0, with $f_0 = 6\pi\eta R_h$ (assuming 0.2 mg/mL hydration).

14 100, $s = 1.91$ S (Van Holde, 1975)]. In order to calculate the frictional coefficients for each protein, we determined their partial specific volumes (ν_{exp}) by carrying out sedimentation equilibrium measurements (Figure 2) so that the equilibration equation (eq 2) could be solved for ν_{exp}. The exact molecular weights of p9^{cksphy} and p13^{suc1}, which are required to solve eq 2, were obtained from electrospray mass-spectrometry determinations. The data are summarized in Table 1. Knowing the values of s, ν_{exp}, and M_r, the frictional coefficients of the proteins were found to be 3.76×10^{-8} g/s for p9^{cksphy} and 4.11×10^{-8} g/s for p13^{suc1}. These values are above the frictional coefficient (f_0) expected for spherical cks monomers (Table 1). Taken together, the small s and large f values obtained in this part of the study indicate that both p9^{cksphy} and p13^{suc1} have an elongated shape in solution. To estimate by how much the cks proteins deviated from being spherical, we calculated the shape factor (F) for each protein (Table 1). This factor, which is defined by $F = f/f_0$, is related to the axial ratio (a/b) of the two possible ellipsoids (oblate and prolate) which could represent the molecular envelope of the proteins (Scheraga, 1961).

(ii) Estimating the Size and Shape of the Molecular Envelope. The previously reported SAXS measurements on the monomeric p9^{cksphy} and p13^{suc1} proteins (Birck *et al*., 1995) demonstrated the monodispersity of the protein solution and yielded the values of the radius of gyration for each protein, 15.8 Å ± 0.4 Å for p9^{cksphy} and 16.8 Å ± 0.4 Å for p13^{suc1}. The formulation of the R_g value for prolate or oblate ellipsoids together with the shape factor provided by the ultracentrifugation data allowed the calculation of the dimensions of these ellipsoids (Mittelbach, 1964). We found that either envelope is as inappropriate as the spherical one to describe the shape of monomeric p9^{cksphy} and p13^{suc1} proteins in solution: only a single α-helix would suit the molecular envelope described by the prolate ellipsoid.

Given that neither the spherical nor the ellipsoidal envelopes provided a good fit to our biophysical data, we next examined whether the published crystal structures of the p9^{ckshs2} and p13^{suc1} proteins would do so. Taking into account the 62% sequence identity between the p9^{cksphy} and p9^{ckshs2} proteins (Figure 1), we used the p9^{ckshs2} protein coordinates (Parge *et al*., 1993), kindly provided by J. Tainer and co-workers, to deduce the molecular envelope. Each p9^{ckshs2} subunit of the dimer has an elongated C-terminal moiety (Figure 3A), and its envelope was defined by a sphere of radius 15 Å that englobes the globular moiety (residues 1→59), attached to a prolate ellipsoid of semiaxes $a = 21$ Å and $b = 7$ Å that covers the extended C-terminal part (residues 60→84) (Figure 4). The computed theoretical frictional coefficient of a protein fitted within this molecular envelope (3.80×10^{-8} g/s) was found in excellent agreement with the experimental f determination for p9^{cksphy} (3.76×10^{-8} g/s). Although the radius of gyration calculated from the atomic coordinates of p9^{ckshs2} (17.8 Å) is slightly larger than the experimental R_g value (15.8 ± 0.4 Å), the calculated maximal dimension of the protein monomer (62 Å) is close to the one estimated from the distance distribution function $p(r)$ derived from the experimental SAXS intensities (around 55 Å). All experimental values for p13^{suc1} monomer (R_g = 16.8 ± 0.4 Å, $f = 4.11 \times 10^{-8}$ g/s, d_{max} = 60 Å) are in agreement with a similar topology. The slightly higher values of p13^{suc1} molecular parameters compared to p9^{cksphy} likely account for the sequence insertions in the p13^{suc1} protein. The 19 amino acid insertion at the N-terminal part encodes a long α-helix in p13^{suc1} and increases the size of the globular domain (Endicott *et al*., 1995a).

Finally, small-angle X-ray scattering patterns were calculated from the crystallographic coordinates using the program CRYSOL (Svergun *et al*., 1995). Figure 5A shows, that the experimental intensities obtained with p9^{cksphy} are well fitted by the curve calculated from the p9^{ckshs2} coordinates. Similar calculations were performed from the coordinates of the zinc-promoted p13^{suc1} dimer, kindly provided to us

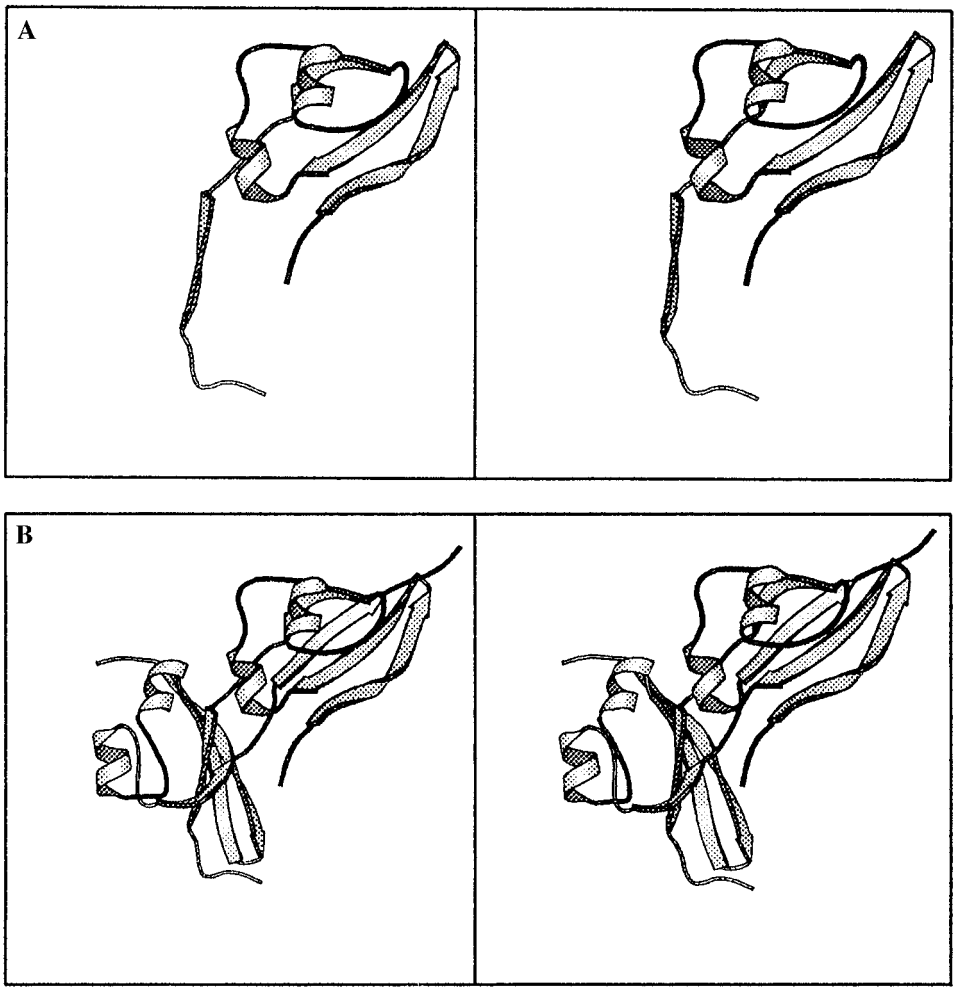

FIGURE 3: Stereoview of (A) the monomeric $p9^{ckshs2}$ subunit fold and (B) the $p9^{ckshs2}$ dimeric fold. The $p9^{ckshs2}$ X-ray structure coordinates (Parge *et al*., 1993) were kindly provided by J. A. Tainer. (A) The monomeric subunit fold shows the extended C-terminal strand. (B) The interlocked dimer results from the C-terminal β-strand exchange between subunits (interchanged residues 60 → 71).

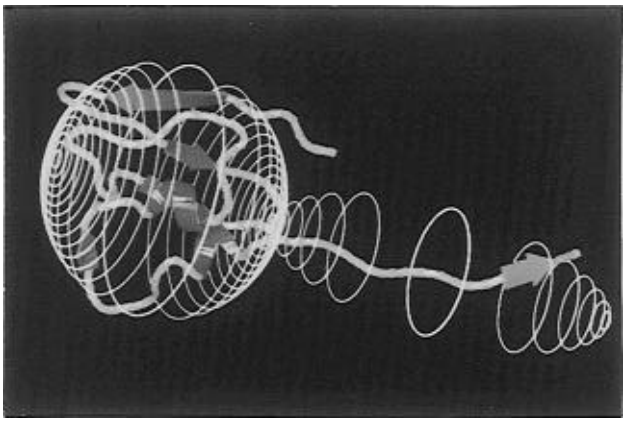

FIGURE 4: Definition of the monomeric $p9^{cksphy}$ molecular envelope. A sphere of radius 15 Å attached to a prolate ellipsoid of semiaxes $a = 21$ Å and $b = 7$ Å englobes the $p9^{cksphy}$ fold. The theoretical frictional coefficient of the protein fitted within this molecular envelope (3.80×10^{-8} g/s) was found to be in excellent agreement with the experimental f determination for $p9^{cksphy}$ (3.76×10^{-8} g/s).

by J. A. Endicott and co-workers. Attempts were made at fitting our experimental scattering pattern of $p13^{suc1}$ with the computed curves of the crystallographic $p13^{suc1}$ globular monomer. It is apparent from Figure 5B that the SAXS data on $p13^{suc1}$ fit much better with the scattering pattern calculated from a nonglobular fold (i.e., $p9^{ckshs2}$) than with the one calculated from the globular fold (i.e., $p13^{suc1}$). These comparisons provide a final support to our contention that both monomers in solution adopt an extended conformation in solution, similar to that observed in crystals of $p9^{ckshs2}$.

Conformational States of Dimeric $p13^{sucl}$: (i) Characterization of Two Independent $p13^{sucl}$ Dimers. We have previously shown, using biochemical methods, that a minor fraction of overexpressed $p13^{suc1}$ was a dimeric species (Birck *et al*., 1995). This raised the question of whether our dimeric $p13^{sucl}$ corresponded to the $p13^{suc1}$ dimers which have been reported by others to form in the presence of zinc ions (Endicott *et al*., 1995a). To test this, we exposed monomeric $p13^{suc1}$ to the conditions in which zinc-promoted dimerization of $p13^{suc1}$ was reported to occur. The resulting molecular species were analyzed by size-exclusion chromatography and SAXS. We found that, in the presence of zinc, $p13^{suc1}$ monomers were quantitatively transformed into dimers. However, SAXS measurements showed that the resulting solution of zinc-promoted $p13^{suc1}$ dimers (at a concentration of 3 mg/mL) was markedly polydispersed. Furthermore, gel-filtration experiments showed that the zinc-promoted $p13^{suc1}$ dimers dissociated back to monomers in the presence of 5 mM EDTA (data not shown). Independent SAXS measurements, performed directly after the addition of EDTA to a solution of zinc-promoted $p13^{suc1}$ dimers, indicated that the resulting monomers were monodispersed, with a radius of gyration of 16.5 Å, indistinguishable from that of "native" monomers (16.8 ± 0.4 Å).

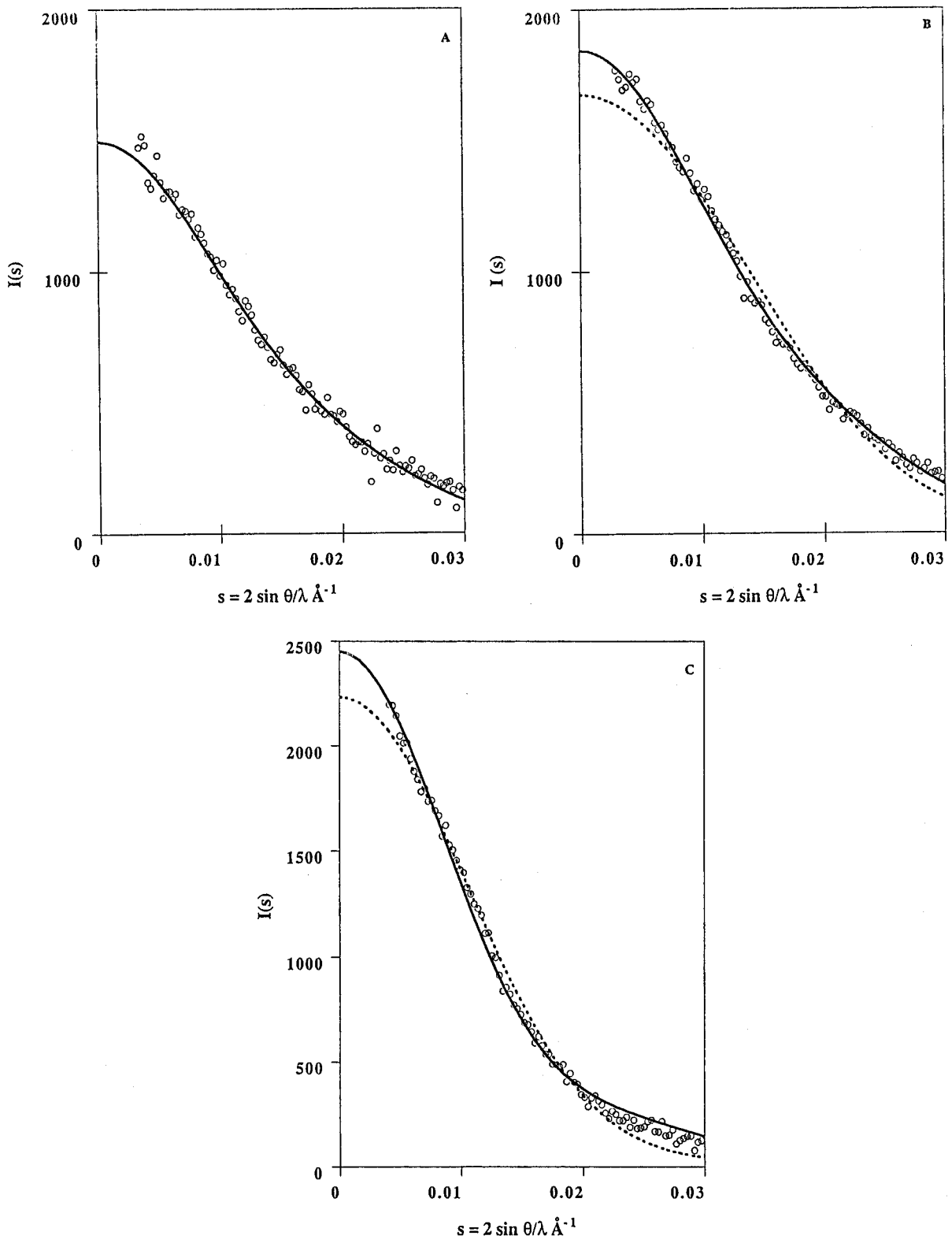

FIGURE 5: Comparison between the scattering patterns calculated from the crystallographic coordinates and the experimental curves. (A) Experimental curve of monomeric $p9^{cksphy}$ (circles); scattering pattern for $p9^{ckshs2}$ calculated from the X-ray structure coordinates of a monomer (continuous line). (B) Experimental curve of monomeric $p13^{suc1}$ (circles); scattering pattern for a globular monomer of $p13^{suc1}$ calculated from the X-ray structure coordinates (dashed line); scattering pattern for $p9^{ckshs2}$ calculated from the X-ray structure coordinates of a monomer (continuous line). (C) Experimental curve of EDTA-insensitive $p13^{suc1}$ dimer (circles); scattering pattern calculated from the coordinates of the zinc-promoted $p13^{suc1}$ dimer (dashed line); scattering pattern calculated from the coordinates of the $p9^{ckshs2}$ dimer (continuous line).

In contrast to the zinc-promoted $p13^{suc1}$ dimers, our "native" $p13^{suc1}$ dimeric form, purified from the pool of overexpressed protein, was insensitive to the addition of zinc and did not dissociate in the presence of EDTA (Figure 6, panel A). In addition, its solutions were monodispersed according to SAXS measurements. The Guinier plot (Figure 7) of the measured SAXS intensities gave a R_g value of 19.6 Å and an apparent molecular mass of 26 700 Da, which is in excellent agreement with the expected value of 26 632 Da. The experimental R_g value is in better agreement with the one calculated, from the X-ray structure coordinates, for the $p9^{ckshs2}$ dimer (20.5 Å) than for the zinc-promoted $p13^{suc1}$

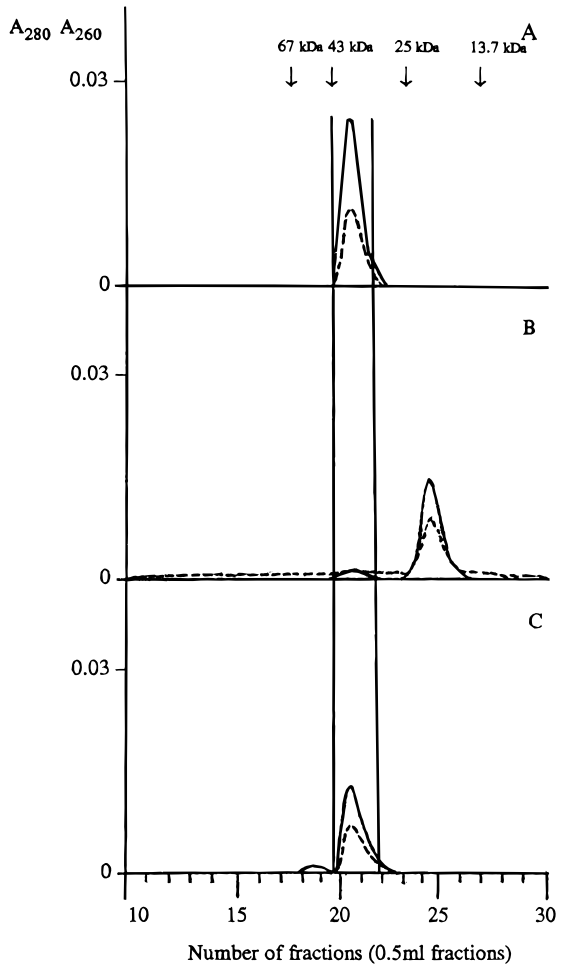

FIGURE 6: Size-exclusion chromatography analysis of p13^{suc1} molecular species. (A) The elution profile of p13^{suc1} dimer (1 mg/mL) is independent of the presence of 5 mM EDTA. (B) After denaturation of the EDTA-insensitive p13^{suc1} dimer, the renatured protein (1 mg/mL) eluted as 95% monomeric species. EDTA-insensitive p13^{suc1} dimeric species was also detectable. (C) The p13^{suc1} monomeric species (1 mg/mL) from panel B formed zinc-promoted p13^{suc1} dimers in the presence of 1 mM $ZnSO_4$. The absorbance was monitored at 280 nm (bold line) and 260 nm (dashed line). Arrows indicate the elution positions of the protein calibration markers. The EDTA-insensitive dimers and the zinc-promoted dimers have identical retention times on the analytical gel-filtration column.

dimers (16.3 Å). The distance distribution function, $p(r)$, gave a maximum molecular dimension of around 60 Å. The experimental curve was finally fitted with the computed scattering pattern of the crystallographic p9^{ckshs2} dimer and with that of the zinc-promoted p13^{suc1} dimer. The general agreement (Figure 5C) is better with the p9^{ckshs2} curve. Our biochemical data strongly argue against the possibility that this EDTA-insensitive p13^{suc1} dimer resembles the zinc-promoted dimer, and all its characteristics fit much better to the dimer topology seen for p9^{ckshs2} (Figure 3B).

(ii) Interconvertibility and Stability of the "Native" Dimer. Given that the "native" p13^{suc1} dimer (EDTA-insensitive p13^{suc1} dimer) was clearly different from the zinc-promoted dimer, and given also that the latter could be reversibly formed from monomers, we wondered what kind of processes mediate the formation of the EDTA-insensitive dimers. This was a particularly intriguing problem, especially in view of the fact that solutions of monomers remained monomeric at all concentrations examined, even after extensive storage in various conditions. This indicated

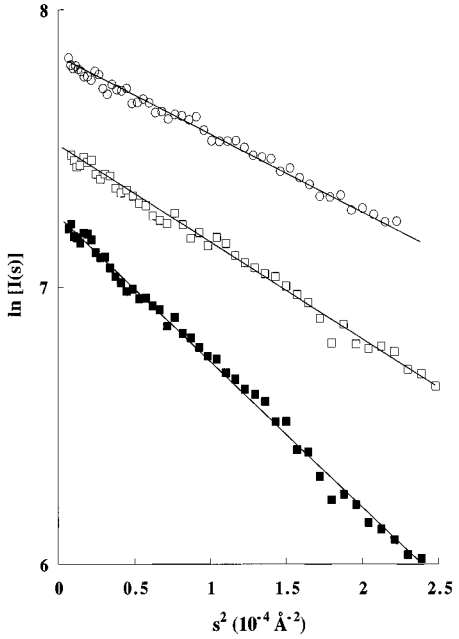

FIGURE 7: Guinier plots of small-angle X-ray scattering data. Symbols: (○) lysozyme at 5.1 mg/mL in 50 mM sodium acetate, pH 4.6; (□) p13^{suc1} monomeric form at 2.5 mg/mL in 50 mM Tris-HCl, pH 8.5, and 250 mM NaCl; (■) p13^{suc1} dimeric form at 2 mg/mL in 50 mM Tris-HCl, pH 8.5, and 250 mM NaCl. The curves were arbitrarily shifted along the vertical axis for the sake of clarity.

that the formation of EDTA-insensitive p13^{suc1} dimer from monomers was not simply due to equilibrium processes. One likely possibility was that the EDTA-insensitive p13^{suc1} dimer formed concomitantly with the monomers during the normal folding pathway of the protein. To test this, EDTA-insensitive p13^{suc1} dimers were denatured in guanidinium chloride, followed by renaturation, and the resulting products were analyzed by analytical gel filtration. The results are shown in Figure 6. The refolding of the denatured EDTA-insensitive p13^{suc1} dimer was nearly quantitative with respect to protein content but provided mainly monomeric species (around 95%) and only about 5% dimers (panel A *versus* panel B). Protein refolding was nearly quantitative, independent of pH in the range 5.5−7.5 and of temperature between 4 and 20 °C. The monomers obtained in this way underwent quantitative zinc-promoted dimerization (panel C), indicating that the p13^{suc1} molecules forming the EDTA-insensitive p13^{suc1} dimer have properties indistinguishable from those of the monomeric p13^{suc1} purified from whole cell lysates. Identical results were obtained when the denaturation−renaturation experiments were performed starting from monomeric p13^{suc1} (data not shown).

Monomeric p9^{cksphy} had a quite different behavior from p13^{suc1} in the presence of zinc ions. By varying the ratios of zinc, salt, and protein, we found that the p9^{cksphy} protein was either soluble and monomeric, or precipitated, and never led to detectable dimeric or higher-order oligomeric species.

DISCUSSION

Small-angle X-ray scattering, analytical ultracentrifugation, mass spectrometry, and analytical gel-filtration data provide all the physico-chemical parameters which define a protein in solution and from which a molecular envelope can be derived. These data allowed us to rule out the possibility that the monomeric p9^{cksphy} and p13^{suc1} proteins may be described as spherical or ellipsoidal globular molecules in

solution. From the biochemical properties of the different molecular species, and from the topologies revealed by X-ray structure determinations, the molecular shape of the *S. pombe* and *P. polycephalum* monomeric proteins satisfying the experimental data was established. All our data indicate that, in solution, monomeric $p9^{cksphy}$ and $p13^{suc1}$ proteins have a nonfolded C-terminal moiety.

Corroborating this conclusion was the excellent agreement between the experimental $p9^{cksphy}$ *f* value and the theoretical *f* value calculated for a protein fitting the molecular envelope of one subunit of $p9^{ckshs2}$ extracted from the crystallographic dimer (Figure 4). On the contrary, the globular monomeric structure, in which strand β4 folds antiparallel to β2 and β3, observed for each $p13^{suc1}$ monomer engaged in the zinc-promoted $p13^{suc1}$ dimer and for the $p9^{ckshs1}$ dimer (Arvai *et al*., 1995), does not fit with any of our experimental results. For example, the R_g values for the globular monomer folds, calculated from the $p13^{suc1}$ and $p9^{ckshs1}$ X-ray structure coordinates (12.9 and 11.9 Å, respectively) are significantly lower than the experimental ones (16.8 ± 0.4 Å and 15.8 ± 0.4 Å for $p13^{suc1}$ and $p9^{cksphy}$ monomers, respectively).

The experimental R_g value for $p9^{cksphy}$ is 2 Å smaller than the R_g value computed for $p9^{ckshs2}$ in which the C-terminal moiety is fully extended (Figure 3A). Such an extended conformation is stabilized by several interactions within the dimer (Parge *et al*., 1993), but it can be reasonably assumed that different conformations may be reached when these 20 residues are exposed to solvent in the monomeric state. This difference in R_g values suggests that the conformation of the C-terminal moiety in the monomeric $p9^{cksphy}$ and $p13^{suc1}$ proteins, although extending from the N-terminal globular core, is not identical to the one observed in the X-ray $p9^{ckshs2}$ dimer. Such a nonglobular fold may explain that crystallization of the monomer, although from a monodispersed solution, may be difficult to achieve.

When applying the experimental conditions leading to the formation of the zinc-promoted $p13^{suc1}$ dimer (Endicott *et al*., 1995a) to the nonglobular $p13^{suc1}$ monomer, we indeed observed, by size-exclusion chromatography, zinc-promoted dimers that could be isolated. However, SAXS measurements showed that the solution of dimers was not monodispersed. These dimers immediately transformed back into monomers in the presence of EDTA, leading to a true monodisperse solution. Since the radius of gyration was identical to that of native nonglobular monomers, this clearly indicates that each globular subunit of the zinc-promoted $p13^{suc1}$ dimers (Endicott *et al*., 1995a) undergoes, upon dimer dissociation, the conformational transition leading to the C-terminal extended fold. This experiment suggests that the monomer globular fold is not thermodynamically favored at pH 7.4 in the presence of 0.2 M sodium chloride. The reversibility of this conformational transition would agree with a thermodynamically controlled process in which the energy barrier between the globular and nonglobular monomer should be low (Baker & Agard, 1994) (Figure 8). Zinc ions seem not only to induce $p13^{suc1}$ dimerization in these conditions but also to promote the conformational transition in which the β4 strand enters the protein core. The fact that dimerization is quantitative indicates that these dimers are more stable than the nonglobular monomers and suggests that dimerization is a means to stabilize the globular monomers. The occurrence of globular folds has so far been observed in crystal structures where cks homologues appear as dimers, stabilized through protein−ligand interactions

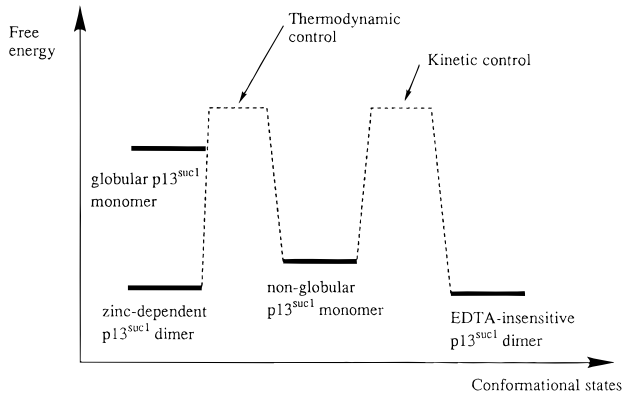

FIGURE 8: Relative energy levels of the different $p13^{suc1}$ molecular forms. The monodispersity and the stability of the respective solutions suggest that nonglobular monomers and EDTA-insensitive dimers represent conformational states of low energies. Zinc ions stabilize the globular fold through dimerization. The reversible transition between nonglobular monomers and zinc-promoted dimers and the exclusive presence of nonglobular monomers in the absence of zinc ions suggest that the energy barrier between nonglobular monomers and folded monomers is low and under thermodynamic control. The parameter that would reduce the energy barrier and allow interconvertibility between nonglobular monomers and EDTA-insensitive dimers is unknown.

involving either zinc ions, for $p13^{suc1}$ (Endicott *et al*., 1995a), or vanadate or phosphate ions, for $p9^{ckshs1}$ (Arvai *et al*., 1995). Our solution studies and the proposal of a low-energy barrier between globular and nonglobular folds are in line with the hypothesis that both sequence-variable regions and environmental changes may affect the conformation of the sequence-conserved β-hinge region from Glu61 to His65 (Arvai *et al*., 1995).

On the basis of SAXS and size-exclusion chromatography, the $p13^{suc1}$ dimer purified from the pool of overexpressed protein was insensitive to EDTA (Figure 6) and was found to be monodispersed in solution (Figure 7). All biophysical and biochemical data suggest that the EDTA-insensitive $p13^{suc1}$ dimer characterized in this work displays the $p9^{ckshs2}$ dimer fold (Figure 3B).

The fact that we could not achieve interconversion between $p13^{suc1}$ monomers and EDTA-insensitive $p13^{suc1}$ dimers was puzzling. One possibility could have been that the dimer formation and stability would depend on a bound and undetected chemical entity provided by the *E. coli* expression system. We thus examined the properties of the $p13^{suc1}$ polypeptide chain through denaturation and renaturation experiments conducted from monomers and from EDTA-insensitive dimers. Starting from either molecular form, refolding reproducibly led to 95% monomers and to 5% EDTA-insensitive dimers that were in all respects, identical to the "naturally" produced species (Figure 6B). Furthermore, the monomeric species obtained after renaturation underwent zinc-promoted dimerization (Figure 6C). This demonstrated that the polypeptide chain forming the EDTA-insensitive $p13^{suc1}$ dimer has, by itself, all intrinsic folding and conformational properties. It also showed that the $p13^{suc1}$ chain may lead, in identical conditions, to stable monomeric and to EDTA-insensitive dimeric forms. Their respective stabilities indicate that a high energy barrier needs to be overcome from interconversion, suggesting that this process might be under kinetic control and therefore irreversible (Baker & Agard, 1994) (Figure 8). Supporting this hypothesis is the formation of 5% dimers from the unfolded $p13^{suc1}$ polypeptide chain. Under these conditions, the energy barrier

between the two defined molecular forms is canceled while refolding proceeds through a kinetically controlled process. The parameter(s) that would decrease this energy barrier, and be relevant under physiological conditions, still need to be identified.

The level of the $p13^{suc1}$ protein remains constant throughout the cell cycle (Brizuela *et al*., 1987). The occurrence of three different molecular forms of $p13^{suc1}$ likely generates different binding sites on the cks protein, as suggested from the X-ray structure analyses (Parge *et al*., 1993; Endicott & Nurse, 1995b; Arvai *et al*., 1995). The evidence given above that they may interconvert under the control of different processes leads to the hypothesis that the resulting oligomeric state may modulate the availability of functional cks at different stages of the cell cycle and may provide an efficient means for the regulation of cdc2 activity.

We previously reported the monodispersity of the monomeric $p9^{cksphy}$ solutions in various media (Birck *et al*., 1995). Attempts to produce higher oligomeric forms in the conditions described for $p9^{ckshs2}$ and $p13^{suc1}$ were unsuccessful. Four residues (Asp23, His26, His40, and Glu91, $p13^{suc1}$ numbering) are involved in the zinc-promoted dimerization process. His40 and Glu91 are the only strictly conserved amino acids within the cks protein family, but interestingly, the $p9^{cksphy}$ protein, which also possesses Asp23, does not form zinc-promoted dimers. This means that the full set of zinc ligands is required to promote the dimer formation which stabilizes the globular fold.

The common molecular form found so far within the cks homologues ($p9^{ckshs1}$, $p9^{ckshs2}$, $p9^{cksphy}$, $p13^{suc1}$) is the monomeric species. The identification and the characterization of the EDTA-insensitive $p13^{suc1}$ dimer reveals that the $p13^{suc1}$ polypeptide chain may, in addition, adopt the two other conformations and molecular assemblies that have been described crystallographically: the $p9^{ckshs2}$ nonglobular fold in the EDTA-insensitive $p13^{suc1}$ dimer and the globular fold in the zinc-promoted $p13^{suc1}$ dimer. The sequence insertions found in the yeast protein thus seem to have no influence in that respect. They may, however, contribute to the main difference between the $p13^{suc1}$ and the $p9^{ckshs2}$ homologues: interconversion between monomers, dimers, and hexamers.

The cks proteins display a surprising range of oligomerization and conformational properties. This brings up the question of the role played by the various cks molecular forms in controlling or tuning the physical associations of cdc2 with its protein partners such as cdc25, wee1, or CAK. Detailed kinetic analyses, solution characterization, and X-ray structure determinations of cks−cdc2 protein complexes should help in unraveling the regulatory mechanism.

ACKNOWLEDGMENT

We thank C. Ebel for help in using the analytical ultracentrifuge at the Institut de Biologie Structurale (Grenoble, France). We are grateful to J. A. Tainer for providing the $p9^{ckshs2}$ and $p9^{ckshs1}$ coordinates and to J. A. Endicott for providing the $p13^{suc1}$ coordinates. We thank D. Svergun for making the program CRYSOL available prior to its general distribution.

REFERENCES

Arvai, A. S., Bourne, Y., Hickey, M. J., & Tainer, J. A. (1995) *J. Mol. Biol. 249*, 835−842.
Azzi, L., Meijer, L., Ostvold, A. C., Lew, J., & Wang, J. H. (1994) *J. Biol. Chem. 269*, 13279−13288.
Baker, D., & Agard, D. A. (1994) *Structure 2*, 907−910.
Basi, G., & Draetta, G. (1995) *Mol. Cell. Biol. 15*, 2028−2036.
Birck, C., Raynaud-Messina, B., & Samama, J. P. (1995) *FEBS Lett. 363*, 145−150.
Bloom, H., Beier, H., & Gross, H. S. (1987) *Electrophoresis 8*, 93−99.
Booher, R. N., Alfa, C. E., Hyams, J. S., & Beach, D. H. (1989) *Cell 58*, 485−497.
Bordas, J., Koch, M. H. J., Clout, P. N., Dorrington, E., Boulin, C., & Gabriel, A. (1980) *J. Phys. E: Sci. Instrum. 13*, 938−944.
Brizuela, L., Draetta, G., & Beach, D. (1987) *EMBO J. 6*, 3507−3514.
Brizuela, L., Draetta, G., & Beach, D. (1989) *Proc. Natl. Acad. Sci.U.S.A. 86*, 4362−4366.
Cantor, C. R., & Schimmel, P. R. (1980) *Biophysical chemistry II*, pp 555−570, W. H. Freeman and Co., New York.
Colas, P., Serras, F., & Van Loon, A. E. (1993) *Int. J. Dev. Biol. 37*, 589−594.
Depautex, C., Desvignes, C., Leboucher, P., Lemonnier, M., Dagneaux, D., Benoit, J. P., & Vachette, P. (1987) LURE Annual Report, p 75, Paris-Sud University, Paris.
Desai, D., Gu, Y., & Morgan, D. O. (1992) *Mol. Biol. Cell. 3*, 571−582.
Draetta, G. (1993) *Trends Cell Biol. 3*, 287−289.
Draetta, G., & Beach, D. (1988) *Cell 54*, 17−26.
Dunphy, W. G. (1994) *Trends Cell Biol. 4*, 202−207.
Dunphy, W. G., & Newport, J. W. (1989) *Cell 58*, 181−191.
Endicott, J. A., & Nurse, P. (1995b) *Structure 3*, 321−325.
Endicott, J. A., Noble, M. E., Garman, E. F., Brown, N., Rasmussen, B., Nurse, P., & Johnson, L. N. (1995a) *EMBO J. 14*, 1004−1014.
Goldberg, M. E., Rudolph, R., & Jaenicke, R. (1991) *Biochemistry 30*, 2790−2797.
Guinier, A., & Fournet, G. (1955) *Small-angle X-ray scattering*, Wiley, New York.
Hadwiger, J. A., Wittenberg, C., Mendenhall, M. D., & Reed, S. I. (1989) *Mol. Cell. Biol. 9*, 2034−2041.
Hayles, J., Beach, D., Durkacz, B., & Nurse, P. (1986a) *Mol. Gen. Genet. 202*, 291−293.
Hayles, J., Aves, S., & Nurse, P. (1986b) *EMBO J.5*, 3373−3379.
Hindley, J., Phear, G., Stein, M., & Beach, D. (1987) *Mol. Cell. Biol. 7*, 504−511.
John, P. C. L., Sek, F. J., & Hayles, J. (1991) *Protoplasma 161*, 70−74.
King, R. W., Jackson, P. K., & Kirchner, M. W. (1994) *Cell 79*, 563−571.
Kusubata, M., Tokui, T., Matsuoka, Y., Okumura, E., Tachibana, K., Hisanaga, S., Kishimoto, H., Kamijo, M., Ohba, Y., Tsujimura, K., Yatanis, R., & Inagaki, M. (1992) *J. Biol. Chem. 267*, 20937−20942.
Laemmli, U. K. (1970) *Nature* (*London*) *227*, 680−685.
Mittelbach, P. (1964) Zur Röntgenkleinwinkelstreuung verdünter kolloider systeme. VIII *Acta Phys. Austriaca 19*, 53−102.
Moreno, S., Hayles, J., & Nurse, P. (1989) *Cell 58*, 361−372.
Parge, H. E., Arvai, A. S., Murtari, D. J., Reed, S. I., & Tainer, J. A. (1993) *Science 262*, 387−395.
Pines, J. (1993) *Trends Biochem. Sci. 18*, 195−197.
Richardson,H. E., Stueland, C. S., Thomas, J., Russel, P., & Reed, S. I. (1990) *Genes Dev. 4*, 1332−1344.
Scheraga, H. A. (1961) *Protein Structure*, Academic Press, New York.
Solomon, M. J., Glotzer, M., Lee, T. H., Philippe, M., & Kirschner, M. W. (1990) *Cell 63*, 1013−1024.
Svergun, D. I. (1992) *J. Appl. Crystallogr. 25*, 495−503.
Svergun, D. I., Semenyuk, A. V., & Feigin, L. A. (1988) *Acta Crystallogr. A44*, 244−250.
Svergun, D., Barberato, C., & Koch, M. H. J. (1995) *J. Appl. Crystallogr. 28*, 768−773.
Van Holde, K. E. (1975) In *Proteins (3rd Ed.)* (Neurath, H., & Hill, R., Eds.) Vol. 1, p 228, Academic Press, New York.

BI952199B